BENEFICIAL CONTROL OF REDUNDANT ELECTRIC DRIVES IN AVIATION

Dirk Fischer*, Robert Rohn*, Regine Mallwitz*
* Institute for Electrical Machines, Traction and Drives (IMAB), TU Braunschweig, Germany

1. INTRODUCTION

Electric Aviation is nowadays a new and highly emergent topic. A lot of concepts are pending and first prototypes are being built. The electric propulsion system has some heavy requirements - for the electric aircraft of the future is has to be powerful, lightweight and especially safe. Today's turbines have a high reliability, but for the case of a failure, especially in multi-engine aircraft there is a power reserve within the remaining turbines. There are standardized power levels for the One-Engine-Inoperative (OEI) such as the 30-seconds OEI, ensuring enough power to finish a critical maneuver as take-off or landing [1]. This leads to an over-sizing in thrust, with a small count of engines up to $100\,\%$. Anyway, the loss of an engine always has a bad impact on flight performance.

The standard three-phase motor and inverter topology as in FIG. 1 has just enough phases to provide a rotary field - the use of multi-phase motors gives more degrees of freedom, enabling a continuing rotary field with the loss of one or more faulted phases. This comes with a power derating, but still is a great opportunity for lowering over-sizing in the design process.

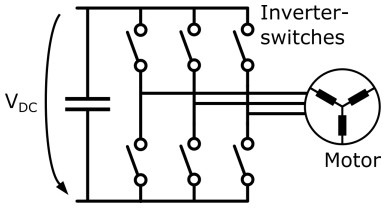

FIG 1. Basic Drive System, consisting of Inverter and Motor

A current approach in electric aviation is distributed electric propulsion, exploiting positive benefits of the usage of multiple engine units across the wing. With a high number of engines, the over-sizing for an OEI can be reduced as well. These concepts combine easily, minimizing the effects of OEI.

A lot of work has been done in analyzing fault behavior of electric multi-phase motors and inverters. An explanation to the use of different phase numbers is given in [2]. It shows possible short-time overrating in the faulted state due to temperature capacity and gives an overview on fault operation quality due to the harmonic spectrum of 5-, 6-, 7- and 9-phase electric motors. An approach to detect faults quickly and different strategies to handle and optimize operating performance in a given multi-phase motor is presented in [3]. A general classification approach, independent from fault tolerance, is given in [4]. Different phase counts and arrangements are set up and analyzed. It is stated that multiple-of-three motors have a beneficial harmonic spectrum since multiple-of-three harmonics are eliminated.

An advantage of fault-tolerant drives is that they offer a redundancy without penalty in design. The use of multi-phase motors and inverters can be seen as paralleling of phases in the most simple version, leading to a proportional scaled power with increasing phases. Hence, there is no power deficit during normal operating conditions.

Special arrangements of phases, starting with the standard three-phase system, offer furthermore possibilities of a higher power outcome due to the manipulation of voltage references. This paper presents the benefits in power outcome due to specific control of redundant, multi-phase systems and compares different topologies.

2. DERIVING THREE-PHASE CARRIER BASED MODULATION

The inverter is used to induce a voltage to the electric motor, resulting in a current and torque. With a higher voltage, higher currents and power outcome are the results. To apply a modulated voltage waveform with an inverter, pulse width modulation (PWM) is the method of choice. The inverter has a DC-Link voltage of V_{DC}, referred to a set and defined midpoint voltage of $0\,V$ this means the voltages $\pm\frac{V_{DC}}{2}$ can be applied with the semiconductor switches to the AC legs of the inverter. The desired output voltages u_v, u_w, u_z are modulated as the mean value of the switched voltage $\pm\frac{V_{DC}}{2}$. To obtain a sufficient quality of the modulated waveform, the switching frequency f_{sw} has to be much higher than the fundamental frequency of the modulated waveform. FIG. 2 and 3 clarify the method. As the electric motor connected to the inverter has inductive behavior, the PWM is intrinsically filtered. What remains is a current in the desired waveform and a small ripple current with the frequency f_{sw}.

2.1. Obtaining a carrier modulation

Usually, the desired voltage is a sine wave. To obtain the correct switching timing, a modulation strategy is needed. A common method is the sine-triangle-PWM comparison [5]. A triangle carrier signal is compared with the reference signal, containing the desired waveform. It has a much higher frequency, at least

©2021

doi: 10.25967/550212

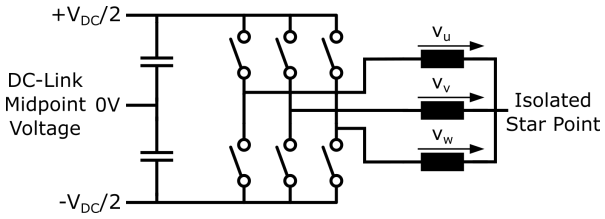

FIG 2. Reference and AC Voltages

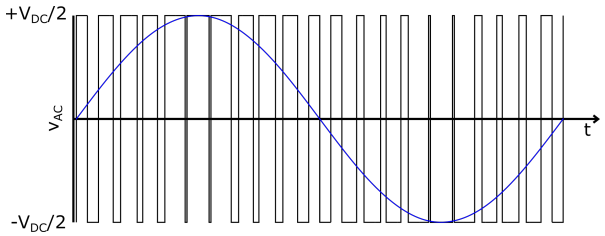

FIG 3. Basic Pulse Width Modulation, switched voltage (—) and modulated voltage (—)

ten times, resulting in the switching frequency f_{sw}. If the reference signal has a higher amplitude than the carrier signal, the output voltage is switched to $v_{AC} = +\frac{V_{DC}}{2}$, if it is lower, the output is switched to $v_{AC} = -\frac{V_{DC}}{2}$. This is plotted exemplary in FIG. 4. Using normalized signals, the modulation index m can be adjusted by a lower amplitude of the reference signal, leading to smaller mean values in the modulated output voltage. The maximum modulation index m for linear sine wave is $m_1 = 1$, higher values lead to a nonlinear waveform, approaching block commutation at $m = \infty$. Using this basic modulation of a single phase, the maximum output voltage is

$$v_{AC,1,peak} = \frac{V_{DC}}{2} \cdot m_{max,1} = \frac{V_{DC}}{2} \tag{1}$$

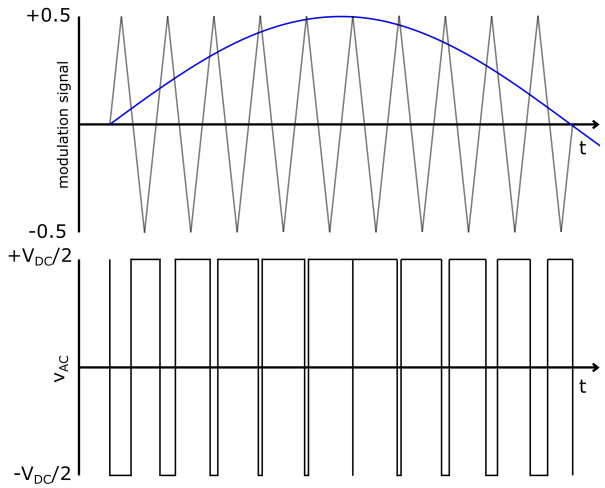

FIG 4. Sine-Triangle-PWM comparison

2.2. Three-Phase Modulation

Extending the carrier based modulation to three phases is simple by paralleling and symmetrically phase shifting three independent systems. The characteristics remain the same.

By using a non-earthed, three phase system like an electric motor with an isolated star point, it is possible to increase the phase voltage without additional DC-Link voltage. In the single-phase system, the voltage is referred to the DC-Link midpoint voltage of $0\,V$. In a multi-phase system, the applied voltages are always phase-to-phase voltages, the reference voltage of the single phases can be different to the DC-Link midpoint, as long as it stays isolated from it.

The isolated star point does not necessarily match the $0\,V$ level of the DC-Link midpoint voltage. It can be manipulated in a way, that the phase voltages have a higher voltage utilization compared to EQ. 1. Since each phase leg can be switch to either $v_{AC} = +\frac{V_{DC}}{2}$ or $v_{AC} = -\frac{V_{DC}}{2}$, the full DC-Link voltage V_{DC} can be applied between two phases. Assumed, the star point voltage can be freely chosen, this leads to a positioning of the DC-Link voltage between the oscillating phase voltages as shown in FIG. 5a.

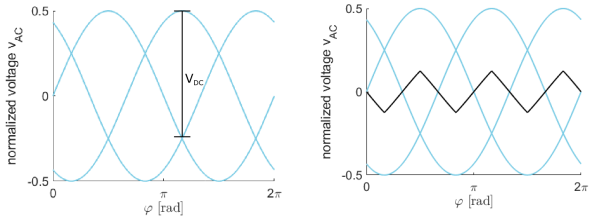

(a) DC-Link Voltage Positioning, Normalized Reference Voltages v_u, v_v, v_w (—)

(b) Star Point Voltage Shifting, Normalized Reference Voltages v_u, v_v, v_w (—), Normalized Offset Voltage V_o (—)

FIG 5. Three-Phase System

To enable this positioning of the DC-Link voltage, at first the midpoint of the phase voltages has to be known. It is placed in the middle of the desired output voltages v_U, v_V and v_W. It can be determined by examining maximum and minimum phase leg voltage at each angle and calculating its midpoint by adding and dividing them by two. The result is the offset of star point voltage as shown in FIG. 5b. Its calculation is given in EQ. 2.

$$V_o = \frac{max(v_u, v_v, v_w) + min(v_u, v_v, v_w)}{2} \tag{2}$$

To apply this offset to the star point, it has to be subtracted from the original reference signals for v_u, v_v and v_e. Since the star point voltage results by superposition of the phase voltages, this leads to an injection of the desired voltage. EQ. 3 shows the calculation of the new reference signals $v_{u,3}, v_{v,3}, v_{w,3}$. A plot is given in FIG. 6.

$$\begin{aligned} v_{u,3} &= v_u - V_o \\ v_{v,3} &= v_v - V_o \\ v_{w,3} &= v_w - V_o \end{aligned} \tag{3}$$

©2021

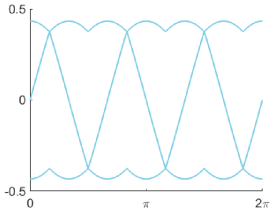

FIG 6. Modulation Signals of Three-Phase System $v_{u,3}, v_{v,3}, v_{w,3}$, m=1 (—)

With the modulation factor $m = 1$, the output voltage $v_{AC,3,peak}$ does not change, but the changed reference gives the option to apply a maximum modulation factor $m_{max,3} > 1$. In the points of maximum modulation (in FIG. 5b: $\varphi = \frac{\pi}{6}, \frac{3\pi}{6}, \ldots$), where star point voltage is the highest, increased voltage gain factor is $\frac{4}{3}$. In the area between these peaks, maximum possible modulation is lower, with a minimum in the points where maximum and minimum sine values are equal spaced, leading to a zero offset in the neutral point shifting (in FIG. 5b: $\varphi = 0, \frac{\pi}{3}, \frac{2\pi}{3}, \ldots$). This corresponds to the maximum over-modulation factor without non-linearity.
EQ. 4 gives a rule to calculate the maximum phase leg voltage, referred to the star point.

(4)
$$v_{max,pp} = \left(\max \left(\max_{n \in N}(v_n(\varphi)) - \min_{n \in N}(v_n(\varphi)) \right) \right)^{-1}$$
$$N = \{u, v, w\}$$
$$\forall \varphi : V_o(\varphi) = 0$$

By inserting normalized voltage amplitudes, the maximum over-modulation factor can be determined. With the reference voltages of EQ. 3 this gives the over-modulation factor $m_{max,3}$.

(5)
$$m_{max,3} = \left(\frac{1}{2} \cdot sin\left(\frac{\pi}{3}\right) - \frac{1}{2} \cdot sin\left(\frac{\pi}{3} - \frac{2\pi}{3}\right) \right)^{-1} = sin\left(\frac{\pi}{3}\right)^{-1} \approx 1.155$$

The maximum output voltage is given by the DC-Link voltage and the possible over-modulation factor.

(6)
$$v_{AC,3,peak} = \frac{V_{DC}}{2} \cdot m_{max,3} \approx 0.577 \cdot V_{DC}$$

3. MULTI-PHASE MODULATION

The method of using an offset function to determine and manipulate a desired star point voltage can be extended to various multi-phase systems. In this chapter, the offset functions, modulations signals and maximum modulation factors for a series of multi-phase systems is examined. At first, different multiple-of-three-phase system are analyzed. They offer a beneficial harmonic suppression and due to their similarity to three-phase systems, they are relatively easy to use. Then a five-phase system is described exemplary to show the expandability of the methodology.

3.1. Six-Phase Symmetrical System

The Six-Phase Symmetrical System as shown in FIG. 7 has a phase shift of $\frac{\pi}{3}$ between each phase leg. According to [4], it has an identical harmonic spectrum as the three-phase motor. In case of a single phase failure, it can back up to be driven as a three-phase system, leaving two healthy and one faulty phase open.
The offset function to manipulate the modulated star point can be extended with the additional phases x, y and z.

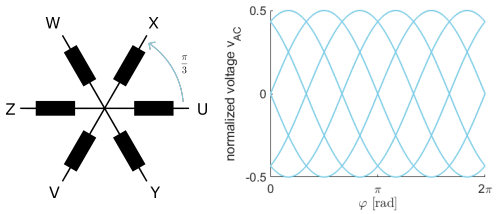

FIG 7. Six-Phase Symmetrical System with normalized Phase Voltages $v_u ... v_z$ (—)

(7)
$$V_{o,6} = \left(\frac{\max_{n \in N}(v_n) + \min_{n \in N}(v_n)}{2} \right)$$
$$N = \{u, v, w, x, y, z\}$$

A characteristic of the sine wave is to have the inverted amplitude at a phase shift of π, $sin(\varphi) = -sin(\varphi + \pi)$. This takes place at an integer multiple of the phase leg shifting of $\frac{\pi}{3}$, what leads to uniform distances of the modulated voltages from the star point. Hence, EQ. 7 gives no offset to add to the modulation signal. EQ. 4 can be expanded to six phases according to EQ. 8:

(8)
$$v_{max,6,pp} = \left(\max \left(\max_{n \in N}(v_n(\varphi)) - \min_{n \in N}(v_n(\varphi)) \right) \right)^{-1}$$
$$N = \{u, v, w, x, y, z\}$$
$$\forall \varphi : V_o(\varphi) = 0$$

It gives a maximum modulation factor of $m_{max,6,sym} = 1$ due to the non-existing offset voltage. FIG. **??** shows the corresponding reference voltages and offset voltage V_o. Since this does not enable the over-modulation as in SEC. 2.2, the maximum output voltage is

(9)
$$v_{AC,6,sym,peak} = \frac{V_{DC}}{2}$$

©2021

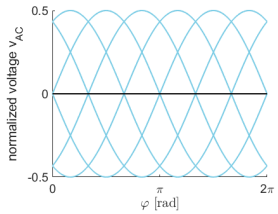

FIG 8. Six-Phase Symmetrical System with normalized Phase Voltages $v_u ... v_z$ (—) and Offset Function V_o (—)

3.2. Six-Phase Asymmetrical System

The Six-Phase asymmetrical system has a non-uniform distribution of its phase legs. Two phase angles of $\varphi_1 = \frac{\pi}{6}$ and $\varphi_2 = \frac{\pi}{2}$ exist. Shifted voltages and phase arrangement are shown in FIG. 9. This asymmetric shifting leads to an improved harmonic spectrum, since it suppresses more harmonics, compared to the symmetric system [6]. As stated in SEC. 3.1, a single phase fault can be handled by using it as a three-phase motor.

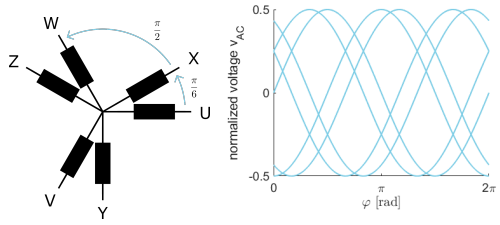

FIG 9. Six-Phase Asymmetrical System with normalized Phase Voltages $v_u ... v_z$ (—)

The disadvantageous symmetric at SEC. 3.1 does not apply for the asymmetric system, leading to a possible non-zero star point shifting. The adapted offset function is the same as EQ. 7. The difference is in the modulation signals $v_u ... v_z$.

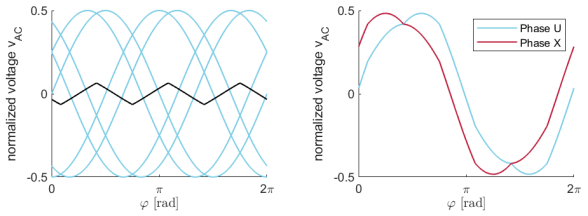

(a) Six-Phase Asymmetrical System with normalized Phase Voltages $v_u ... v_z$ (—) and Offset Function V_o (—)

(b) Modulation Signal, m=1, Phase U (—) and Phase X (—)

FIG 10. Six-Phase Asymmetrical System

FIG. 10a shows the possible star point shifting. It is similar to the three phase shifting, but centered with its maximum between the $\frac{\pi}{6}$ shifted phases. This leads to a lower maximum value, since it does not fit the peak values of the sine waves. The zero crossings of the modified neutral point are located at $\frac{\pi}{4}, \frac{7\pi}{12}, \frac{11\pi}{12}$... and have a corresponding maximum sine amplitude of $sin(\frac{5\pi}{12})$ and minimum sine wave $sin(\frac{19\pi}{12})$. With EQ. 8, this leads to a maximum, linear over-modulation of

(10)
$$v_{max,6,pp} = \left(\max \left(\max_{n \in N}(v_n(\varphi)) - \min_{n \in N}(v_n(\varphi)) \right) \right)^{-1}$$
$$N = \{u, v, w, x, y, z\}$$
$$m_{max,6,asym} = \left(\frac{1}{2} \cdot sin\left(\frac{5\pi}{12}\right) - \frac{1}{2} \cdot sin\left(\frac{19\pi}{12}\right) \right)^{-1}$$
$$\approx 1.035$$

With this, the maximum possible voltage in the asymmetric six-phase system is given in EQ. 11.

(11)
$$v_{AC,6,asym,peak} = \frac{V_{DC}}{2} \cdot m_{max,6,asym} \approx 0.518 \cdot V_{DC}$$

3.3. 2x3-Phase Isolated System

The 2x3-Phase Isolated System, sometimes referred as dual stator, is basically two mechanically coupled three phase systems. They have no conducting connection and most importantly, two separated star points. This gives the opportunity to treat the isolated systems separately and induce two different star point offsets. A useful feature is that this arrangement can be fed by two separate inverters, so the system can be built without the need of a customized multi-phase inverter.

The phase shift can be chosen to a symmetric, asymmetric or parallel construction. Also, the principle can be extended to more than two independent three-phase systems. In this case, an asymmetric construction is chosen for better visibility of the plots.

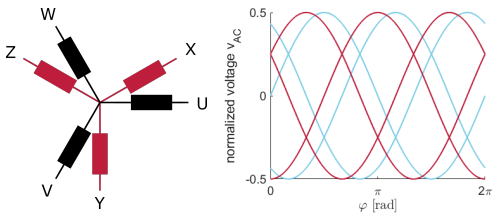

FIG 11. 2x3-Phase Isolated System with normalized Phase Voltages v_u, v_v, v_w (—), v_x, v_y, v_z (—)

To provide two different offset voltages to the isolated star points, the three phase offset function in EQ. 2 has to be calculated two times, regarding to the independent electrical systems. EQ. 12 then gives the following two offset functions $V_{o,1}$ and $V_{o,2}$:

(12)
$$V_{o,1} = \frac{max(v_u, v_v, v_w) + min(v_u, v_v, v_w)}{2}$$
$$V_{o,2} = \frac{max(v_x, v_y, v_z) + min(v_x, v_y, v_z)}{2}$$

The offset functions $V_{o,1}$ and $V_{o,2}$ are subtracted from the modulation signals, giving two electrical indepen-

©2021

dent three-phase systems, each with the properties of a single three-phase system. FIG. 12 shows the two shifted systems with their corresponding offset functions (12a) and the independent modulation signals (12b).

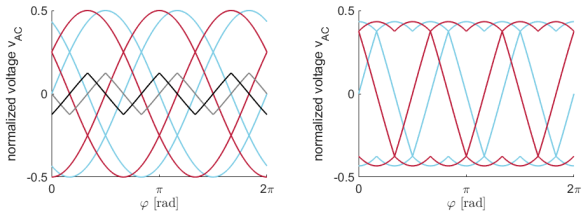

(a) 2x3 System with normalized Phase Voltages $v_u ... v_z$ (—/ —) and Offset Functions $V_{o,1}$, $V_{o,2}$ (—)

(b) Modulation Signal, m=1, Phase U,V,W (—) and Phase X,Y,Z (—)

FIG 12. 2x3-Phase Isolated System

(13)

$$v_{max,2x3,pp} = \left(\max \left(\max_{n \in N}(v_n(\varphi)) - \min_{n \in N}(v_n(\varphi)) \right) \right)^{-1}$$

$$N = \{u, v, w, x, y, z\}$$

$$m_{max,2x3} = \left(\frac{1}{2} \cdot sin\left(\frac{\pi}{3}\right) - \frac{1}{2} \cdot sin\left(\frac{\pi}{3} - \frac{2\pi}{3}\right) \right)^{-1}$$

$$\approx 1.155$$

Due to its similarity to the three-phase system, EQ. 4 gives the same maximum modulation factor of $m_{max,2x3} = 1.155$ and resulting voltage utilization of

(14) $$v_{AC,2x3,peak} = \frac{V_{DC}}{2} \cdot m_{max,2x3} \approx 0.577 \cdot V_{DC}$$

3.4. Five-Phase System

The Five-Phase System as in FIG. 13 has an equal phase leg distribution with an angle of $\varphi = \frac{2\pi}{5}$ between each leg. With the lowest existing harmonic being of 9th order, except of the fundamental wave, it has a very good harmonic spectrum, but by the cost of a high phase number. In the fault case, a rotary field can still be induced due to the five independent currents, or four in case of a single fault, but this comes with a reduced torque and a high torque ripple due to the unsymmetrical field distribution of the remaining phases.

Due to its odd number of phases, there is no symmetry in the sine modulation, leading to a non-zero offset function.

EQ. 7 can easily be adapted to EQ. 15:

(15) $$V_{o,5} = -\left(\frac{\max_{n \in N}(v_n) + \min_{n \in N}(v_n)}{2} \right)$$

$$N = \{u, v, w, x, y\}$$

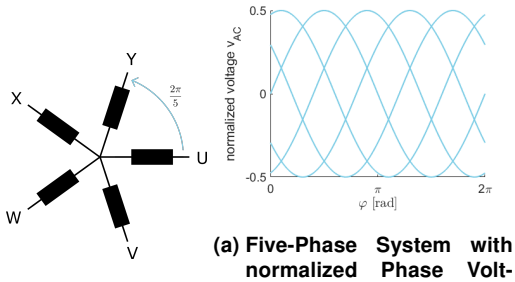

(a) Five-Phase System with normalized Phase Voltages $v_u ... v_y$ (—)

FIG 13. Five-Phase System

The calculated offset can be subtracted from the reference to obtain the modulation signal in FIG. 14b.

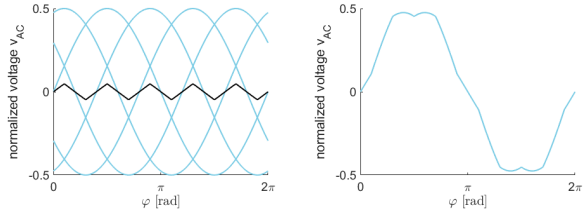

(a) Five-Phase System with normalized Phase Voltages $v_u ... v_y$ (—) and Offset Function V_o (—)

(b) Modulation Signal, m=1, Phase U(—)

FIG 14. Five-Phase System

Star point offset has its zero crossings at multiples of $\varphi = \frac{\pi}{5}$. Extending EQ. 4 to five phases and insert $\varphi = \frac{\pi}{5}$, the maximum over-modulation factor is calculated by EQ. 16 using normalized voltages.

(16)

$$v_{max,pp} = \left(\max \left(\max_{n \in N}(v_n(\varphi)) - \min_{n \in N}(v_n(\varphi)) \right) \right)^{-1}$$

$$N = \{u, v, w, x, y\}$$

$$m_{max,5} = \left(\frac{1}{2} \cdot sin\left(\frac{3\pi}{5}\right) - \frac{1}{2} \cdot sin\left(\frac{7\pi}{5}\right) \right)^{-1} = 1.052$$

Finally, the maximum output voltage can be calculated to

(17) $$v_{AC,5,peak} = \frac{V_{DC}}{2} \cdot m_{max,5} \approx 0.526 \cdot V_{DC}$$

3.5. System Comparison

The offset functions of the different systems lead to to various maximum modulation factors m_{max} and resulting voltage utilization. TAB. 1 gives an overview on the discussed topologies. The highest m_{max} and corresponding max. v_{AC} applies to the Three-Phase System as well as the 2x3 Phase System with a maximum phase voltage of $v_{AC,max} = 0.577 \cdot V_{DC}$. This gives the advantage to implement the highest voltage utilization to different topologies, since the principle of an isolated star-point is extendable to more elemen-

©2021

tary motors and every angle φ between the phase legs.

TAB 1. Multi-Phase Systems Overview

Description	Phases	m_{max}	max. v_{AC}
Single Phase	1	1	$0.5 \cdot V_{DC}$
Three Phase	3	1.155	$0.577 \cdot V_{DC}$
Six Phase Symmetric	6	1	$0.5 \cdot V_{DC}$
Six Phase Asymmetric	6	1.035	$0.518 \cdot V_{DC}$
2x3 Phase	6	1.155	$0.577 \cdot V_{DC}$
Five Phase	5	1.052	$0.526 \cdot V_{DC}$
Seven Phase	7	1.026	$0.513 \cdot V_{DC}$
Nine Phase	9	1.015	$0.508 \cdot V_{DC}$

4. VALIDATION OF CONTROL STRATEGY

In this chapter, the modulation strategies are verified. A model of an inverter is implemented in a Simscape (MATLAB/Simulink) environment. It is connected to several RL-loads, representing a basic layout of a multi-phase motor. The parameters of the simulation are given in TAB. 2. A schematic of the circuit is given in FIG. 15.

TAB 2. Multi-Phase Systems Overview

DC-Link voltage	$V_{DC} = 1000\,V$
Load resistance	$R = 1\,\Omega$
Load inductance	$L = 200\,\mu H$
Switching frequency	$f_{sw} = 10\,kHz$

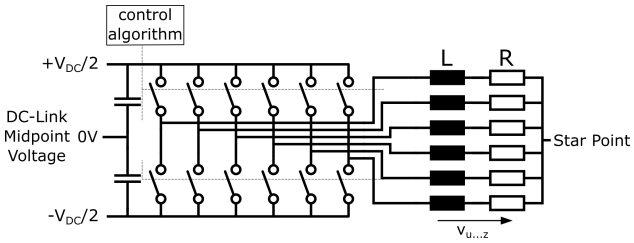

FIG 15. Schematic of the applied Model, Six Phases and connected Star Point

4.1. Three-Phase Modulation

The modulation strategy derived in SEC. 2.2, respectively EQ. 3, is implemented using a signal-triangle comparison, the switches are fed with the resulting pulse patterns. To approve the waveform modulation, in FIG. 16a the phase-leg voltage referred to the DC-midpoint $0\,V$ and to the motor star point is plotted. Since the applied voltage results from the mean value of the switched DC-Link voltage, a moving average filter is used to evaluate the voltage form. The maximum applicable modulation factor $m_{max,3} = 1.155$ is used according to EQ. 5.

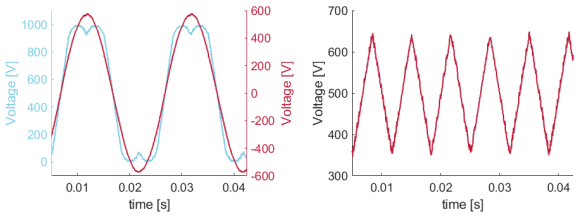

(a) Phase leg voltage, referred to DC-Link midpoint voltage (—) and to star point(—)

(b) Star point voltage

FIG 16. Three-Phase simulation voltage waveforms

Maximum resulting voltage across the load is $V_{max,3} = 0.58 \cdot V_{DC}$, including a small inaccuracy due to averaging of the voltage.

4.2. Six-Phase Symmetrical Modulation

The six-phase symmetrical system can't obtain an star point offset voltage because of its $\frac{\pi}{3}$-symmetry (see SEC. 3.1), resulting in a maximum modulation factor $m_{max,6,sym} = 1$. FIG. 17 gives the phase leg

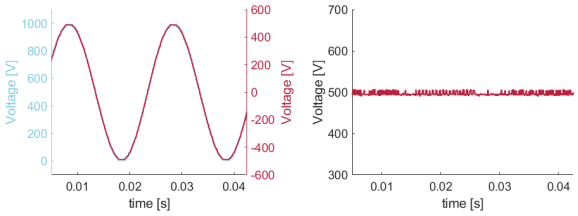

(a) Phase leg voltage, referred to DC-Link midpoint voltage (—) and to star point(—)

(b) Star point voltage

FIG 17. Six-Phase symmetrical simulation voltage waveform

voltages referred to DC-Link midpoint and to the star point. The offset voltage is equivalent to the DC-Link midpoint. This results in an identical voltage waveform with no additional voltage exploitation. Maximum voltage across the load is $V_{max,6,sym} = 0.5 \cdot V_{DC}$.

4.3. Six-Phase Asymmetrical Modulation

The six-phase asymmetrical system has a star point offset voltage (FIG.10) and a modulation factor of $m_{max,6,asym} = 1.035$ according to EQ. 10. This leads to an improved phase leg voltage as shown in FIG. 18.

Phase leg voltage of the asymmetric six-phase system shows a slightly higher voltage waveform referred to the star point than to DC-Link midpoint voltage. The maximum value is $V_{max,6,asym} = 0.517 \cdot V_{DC}$.

©2021

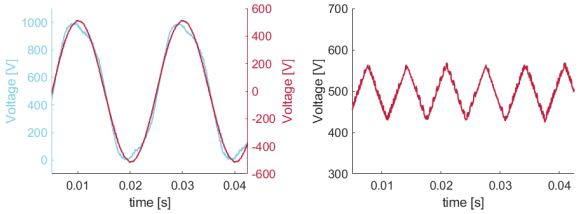

(a) Phase leg voltage, referred to DC-Link midpoint voltage (—) and to star point(—)

(b) Star point voltage

FIG 18. Six-Phase asymmetrical simulation voltage waveform

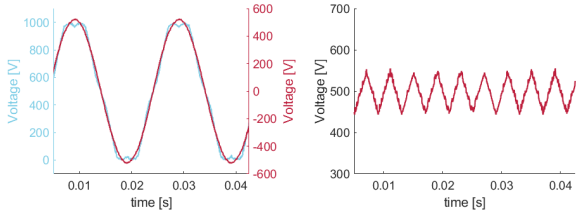

(a) Phase leg voltage, referred to DC-Link midpoint voltage (—) and to star point(—)

(b) Star point voltage

FIG 20. Five-Phase simulation voltage waveform

4.4. 2x3-Phase Isolated System

In the 2x3-phase isolated System, there are two star points separating it into two independent systems. This leads to two different offset voltages and to two coupled, three phase systems. The maximum modulation factor is $m_{max,2x3} = 1.155$ according SEC. 3.3.

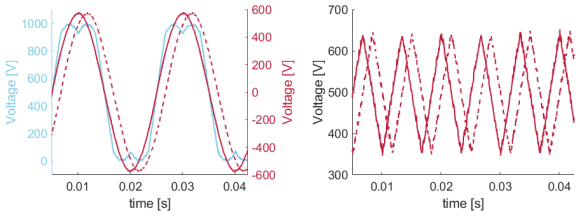

(a) Phase leg voltage, referred to DC-Link midpoint voltage (—) and to star point(—)

(b) Star point voltages

FIG 19. 2x3-Phase simulation voltage waveform

FIG. 19 shows the phase leg voltages of both isolated systems. They are identical to the three-phase waveform in FIG. 16, expect of the second, phase shifted system existing. Maximum voltage across the loads is also the same with $V_{max,2x3} = 0.58 \cdot V_{DC}$. FIG. 19a shows the voltage of Phase U as well as Phase X from both independent Systems. FIG. 19b shows the two independent star-point offset voltages, referred to the DC-Link midpoint voltage.

4.5. Five-Phase System

The five-phase system has an star point offset as shown in FIG. 14 and according to EQ. 16 a maximum modulation factor $m_{max,5} = 1.052$.
FIG. 20 gives the phase leg voltage waveform of the five-phase system. Maximum voltage across the load is $V_{max,5} = 0.526 \cdot V_{DC}$. The star-point voltage offset in FIG. 20, referred to the DC-Link midpoint voltage, is lower than the systems before.

4.6. System Comparison

As shown, the control of different motor topologies can have a noteworthy effect on their applied phase voltage. This higher voltage can be utilized to inject proportional higher motor currents without increased DC-Link voltage. FIG. 21 shows the resulting phase currents of the discussed multi-phase systems normalized to the highest occurring current.

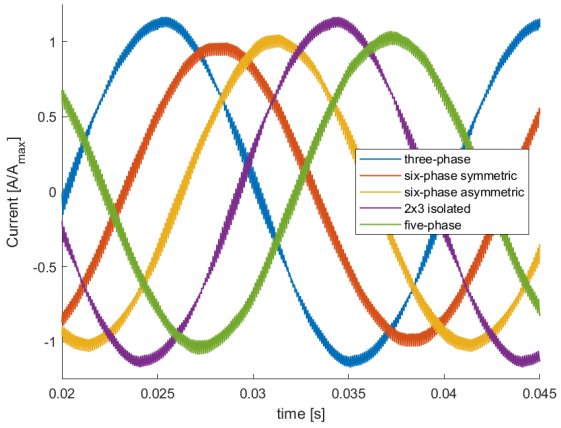

FIG 21. Normalized Phase-Leg Currents of each System Topology

TAB 3. Multi-Phase Systems Overview

Description	m_{max}	$\frac{A}{A_{max}}$	P_{spec}
Three-Phase	1.155	1.155	1.334
Six-Phase Symmetric	1	1	1
Six-Phase Asymmetric	1.035	1.035	1.071
2x3-Phase	1.155	1.155	1.334
Five-Phase	1.052	1.052	1.107
Seven-Phase	1.026	1.026	1.053
Nine-Phase	1.015	1.015	1.030

The higher voltage utilization along with higher currents lead to a higher specific power P_{spec}, square dependent to $m_{max,n}$: $P_{spec} \propto (m_{max,n})^2$.
The higher specific power does not apply totally to a proportional higher power density, since motor and inverter have to be constructed for the applied currents. The voltage insulation in inverter an motor is designed for the DC-Link voltage, so the higher voltage due to

©2021

voltage utilization comes for free, what directly leads to a higher specific power density $\frac{P_{spec}}{m} \propto m_{max,n}$. TAB. 3 compares the discussed systems according to maximum modulation index, resulting current and specific power. The best voltage utilization arises in the three-phase system as well as in the 2x3 isolated system, which offers 50% remaining power in case of a single phase fault. The concept of the isolated star point is expendable to each multiple of three, so that the topology can be used for even more redundancy stages.

5. SUMMARY

After an introduction to the topic of redundant electric drives, the modulation of the basic variant of the three-phase system is derived in detail and the method of DC-Link voltage positioning to over-modulate the phase leg voltage is explained. Formulas for maximum phase leg voltage and star point offset calculation are derived. The method then is extended to a multi-phase approach and applied to different topologies. Resulting voltage references and phase leg voltages are calculated. The results are validated in a simulation to prove their functionality and voltage utilization. Conclusions to an improved power density are drawn.

6. ACKNOWLEDGMENT

The authors thankfully appreciate the German Aerospace Center (DLR) for the promotion of the LuFo VI-1 Project EPROREF.

Contact address:

dirk.fischer@tu-braunschweig.de

References

[1] U.S. Department of Transportation. GUIDANCE FOR 30-SECOND AND 2- MINUTE ONE-ENGINE-INOPERATIVE (OEI) RATINGS FOR ROTORCRAFT TURBINE ENGINES: Advisory Circular AC No 33-7A. 2009.

[2] I. Bolvashenkov, J. Kammermann, S. Willerich and H.-G. Herzog. Comparative Study of Reliability and Fault Tolerance of Multi-Phase Permanent Magnet Synchronous Motors for Safety-Critical Drive Trains. *International Conference on Renewable Energies and Power Quality (ICREPQ'16)*, 2016.

[3] Hisham Magdy Gamal Eldeeb. *Modelling, Control and Post-Fault Operation of Dual Three-phase Drives for Airborne Wind Energy*. Dissertation, Technische Universität München, 2019.

[4] E. A. Klingshirn. High Phase Order Induction Motors - Part I-Description and Theoretical Considerations. *IEEE Transactions on Power Apparatus and Systems*, PAS-102(1):47–53, 1983. DOI: 10.1109/TPAS.1983.317996.

[5] Steffen Bernet. *Selbstgeführte Stromrichter am Gleichspannungszwischenkreis*. Springer, Berlin, Heidelberg, 2012. DOI: 10.1007/978-3-540-68861-7.

[6] Kashif S. Khan, Waqas M. Arshad, and Sami Kanerva. *On performance figures of multiphase machines: ICEM 2008 ; 6 - 9 Sept. 2008, Vilamoura, Portugal*. IEEE, Piscataway, NJ, 2008. ISBN: 9781424417360.

©2021